The Sub-THz Emission of the Human Body Under Physiological Stress

Ksenia A. Baksheeva, Roman V. Ozhegov, Gregory N. Goltsman, Nickolay V. Kinev, Valery P. Koshelets, *Member, IEEE*, Anna Kochnev, Noa Betzalel, Alexander Puzenko, Paul Ben Ishai, and Yuri Feldman

***Abstract*—We present evidence that in the sub-THz frequency band, human skin can be considered as an electromagnetic biometamaterial in which its natural emission is a product of skin tissue geometry and embedded structures. Radiometry was performed on 32 human subjects from 480 to 700 GHz. Concurrently, the subjects were exposed to stress, while heart pulse rate (PS) and galvanic skin response (GSR) were also measured. The results are substantially different from the expected blackbody radiation signal of the skin surface. PS and GSR correlate to the emissivity. Using a simulation model for the skin, we find that the sweat duct is a critical element. The simulated frequency spectra qualitatively match the measured emission spectra and show that our sub-THz emission is modulated by our level of mental stress. This opens avenues for the remote monitoring of the human state.**

***Index Terms*—Black body radiation, human skin emission, sub-THz, sweat ducts.**

I. Introduction

The human body does not present many opportunities for monitoring its vital state. Despite advances in invasive monitoring and diagnosis, medicine is still limited to the same techniques of yesteryears. Excluding medical imagery, the last major innovation in continuous monitoring is the electrocardiogram, introduced in 1895 [1]. The visual impression of the person, together with pulse and skin temperature, is a major component of any diagnosis, a situation that harks back to the days of Hippocrates and Galen. The skin is a major organ of the body [2] and is a source of information. However, there is a conundrum. Any remote technique requires communication—mechanical or electromagnetic—and the human body is rather quiet. Although visual information can be gleaned, it is a long-held view that the human body does not "shine." Beyond blackbody radiation, we do not radiate [3]. Indeed, the human skin temperature of approximately 32 °C leads to equivalent blackbody spectra in the infrared [4]. This has been exploited to expose sick individuals in crowds at airports [5].

We present results demonstrating that the traditional view is not complete. There is also a marked contribution in the sub-THz region. Furthermore, this contribution is sensitive to the physiological state of the subject, opening a remote diagnostic channel.

The lack of data between 100 GHz and the infrared was partly due to the difficulty of performing radiometry experiments in the sub-millimeter (sub-THz) band [6]. Nowadays, modern heterodyne techniques can cover this range in laboratory conditions.

We have conducted a radiometric study of human emissivity around 500 and 507 GHz on 32 volunteers, the preliminary results of which were reported in [7]. In this missive, we provided a full and complete description and discussion. The motivation to measure the emission of the human body in this range was experiments linking the morphology of the eccrine sweat ducts to stress-based variations in the reflection coefficient of the human palm, conducted in the frequency range of 75–430 GHz [8]–[11]. An intriguing finding was the demonstration of circular dichroism [12] in the reflectance of the skin, which is significant because the helical structure of the sweat duct [13], [14] (see Fig. 1) is the only candidate in the epidermis that would cause such. Consequently, one must question would there be an implication on the emission of the human body.

II. Materials and Methods

A. Experimental Setup

The experimental setup is based around a superconducting integrated receiver (SIR) [15], [16] located in a cryostat with liquid helium [15], [17]. The general schematic of the system is presented in Fig. 2. Concurrent supplementary measurements of the galvanic skin response (GSR), skin temperature, and heart

Manuscript received September 5, 2020; revised January 5, 2021 and February 25, 2021; accepted March 5, 2021. Date of publication March 17, 2021; date of current version July 2, 2021. The work of Ksenia A. Baksheeva, Roman V. Ozhegov, Gregory N. Goltsman, Nickolay V. Kinev, and Valery P. Koshelets was supported by the Russian Foundation for Basic Research under Grant 17-29-02354. The SIR development is supported by Russian Science Foundation under Project 19-19-00618. *(Corresponding author: Yuri Feldman.)*

Ksenia A. Baksheeva is with the Moscow Pedagogical State University, 119991 Moscow, Russia (e-mail: baksheeva.kseniya@mail.ru).

Roman V. Ozhegov and Gregory N. Goltsman are with the Moscow Pedagogical State University, 119991 Moscow, Russia, and also with the Moscow Institute of Electronics and Mathematics, National Research University Higher School of Economics, 109028 Moscow, Russia (e-mail: ozhegov_roman@mail.ru; goltsman10@mail.ru).

Nickolay V. Kinev and Valery P. Koshelets are with the Kotel'nikov Institute of Radio Engineering and Electronics, Russian Academy of Sciences, 125009 Moscow, Russia (e-mail: nickolay@hitech.cplire.ru; valery@hitech.cplire.ru).

Anna Kochnev, Noa Betzalel, Alexander Puzenko, and Yuri Feldman are with the Department of Applied Physics, The Hebrew University of Jerusalem, Jerusalem 9190401, Israel (e-mail: anna.kochnev@mail.huji.ac.il; noa.betzalel@mail.huji.ac.il; puzal@mail.huji.ac.il; yurif@mail.huji.ac.il).

Paul Ben Ishai is with the Department of Physics, Ariel University, Ariel 40700, Israel (e-mail: paulbi@ariel.ac.il).

Color versions of one or more figures in this article are available at https://doi.org/10.1109/TTHZ.2021.3066099.

Digital Object Identifier 10.1109/TTHZ.2021.3066099

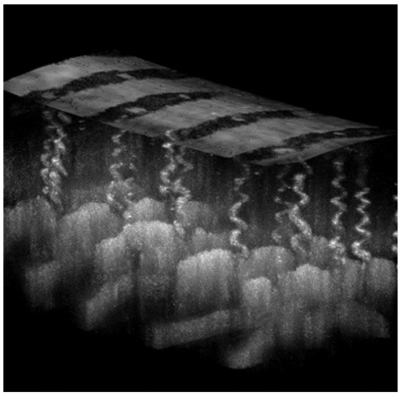

Fig. 1. Optical coherence tomography (OCT) image of the human skin showing the existence of the coiled portion of the sweat duct (Gabor-domain OCT. Image by Jannick P. Rolland, University of Rochester).

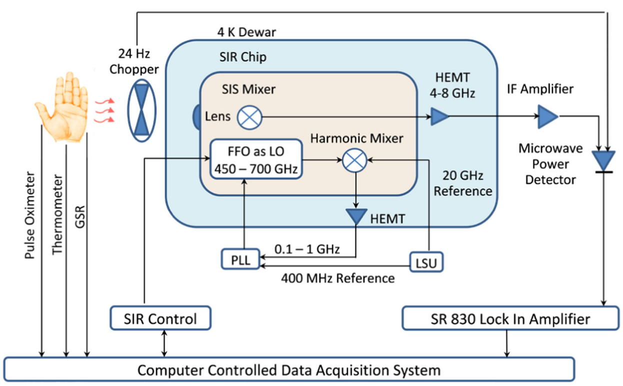

Fig. 2. Schematic of the measuring setup, including a superconducting integrated receiver (SIR), GSR, pulse meter, and skin temperature sensors. The abbreviations in the block diagram are FFO: flux-flow oscillator, a local oscillator in the SIR, IF amplifier: intermediate frequency amplifier, SIS mixer: the superconductor–insulator–superconductor mixer, PLL: phase-locked loop, LSU: local source unit, and HEMT: High-electron mobility transistor.

pulse rate were made using a GSR logger sensor NUL-217, a thermometer DT-670SD, and a pulse oximeter CMS50D, respectively. All of these sensors are connected to the data collection system. The subjects' hand was immobilized in the stand at a distance of 25 cm from the cryostat window. The radiometry signal was modulated by a chopper placed 5 cm from the cryostat window, rotating at 24 Hz.

B. Superconducting Integrated Receiver

The SIR was used to measure the brightness temperature of the subject's skin at 500 and 507 GHz for our entire set of participants. Additionally, spectral measurements in the range 480–700 GHz were carried out on three subjects. Tuning the SIR for each frequency point is a time-consuming process. Therefore, due to time and manpower constraints, only three spectra were measured. The SIR integrates into a 4 × 4 × 0.5 mm^3 chip of a sensitive terahertz range SIS mixer, a highly stable terahertz oscillator, and phase locked by using a harmonic mixer [14], [15]; all these superconducting elements operate at cryogenic temperatures. The SIR is designed to work in the

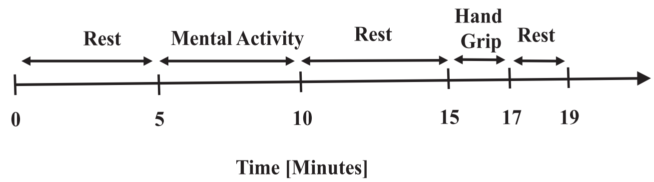

Fig. 3. Measurement protocol: 5 min rest, 5 min of mental stress, 5 min of rest, 2 min of physical stress, and 2 min of rest more.

470–670 GHz frequency range; the noise temperature as low as 120 K, and the IF bandwidth 4–8 GHz was demonstrated [15], [17].

C. Supplementary Signals

GSR is a measurement of the impedance of the skin. Basic electrodermal activity theory holds that the impedance of the skin is influenced by the state of the sweat glands and the sweating process is controlled by the sympathetic nervous system. Consequently, changes in the resistance of the skin can be used as a window to the nervous system and an indication of the psychological and physiological stress. It is widely used in polygraph tests and other psychophysiology measurements. Serving as a widely used measure of stress and nervous excitation, the recording of the GSR signal served as a control signal to verify the experimental protocol indeed induced some level of stress. As such, the correlation of the received SIR signal and the GSR result is an indicative of the effect of stress in the radiometry result. The GSR channel was measured by connecting the electrodes to two fingers' tips on the subject's left hand. A thermometer and a pulse oximeter were also used to monitor the pulse and oxygen content in the blood. These detectors were attached to the subject's left hand. From the heart pulse rate, it is possible to derive heart rate variability (HRV), another well-established indicator of subject stress.

D. Experimental Protocol

A total of 30 out of 42 measurements were conducted under a protocol that began with 5 min of relaxation, followed by 5 min of mental stress. Then, again 5 min of relaxation, followed by 2 min of physical stress and finished off by 2 min of rest (see Fig. 3). The remaining 12 measurements were carried out with a shorter protocol of 5 min of relaxation, followed by 3 min of mental stress, and finished off by another 5 min of relaxation. The subjects were requested to avoid coffee and heavy meals for at least 2 h prior to the experiment and upon arrival were requested to wash their hands with soap, in order to remove hand lotion, if such had been applied. Additionally, they were asked to leave their cell phones outside the measurement room to avoid sudden interrupts and additional noise in the room. Afterward, they were brought into the measurement room where they received a general explanation of the goals and procedures of the experiment that they were about to participate in, which also allowed the subject to adjust and relax to the experimental surroundings. After signing informed consent forms, they were requested to sit comfortably in front of the measurement table and place their left hand in the chassis. The hand was then fixed at the point of focus and additional measurement devices, discussed in the discussed in Section C. Supplementary Signals, were connected as well.

E. Subject Pool

The subjects were recruited from the staff and student body of the Moscow Pedagogical State University. The criteria for participation were that the subjects should be healthy under the age of 40 with no skin complaints. The participants were 19 female and 13 male volunteers ranging between 18 and 37 years of age (average age 23 years) and the protocols were under the approval of the Ethical Committee of Moscow Pedagogical State University, Russia. They were informed regarding the experimental aspects relevant to human health and freely gave their consent.

III. Results

The radiometry experiments show that, at 507 GHz, the emission of the human skin is substantially different from the blackbody signal of the skin temperature for the sample pool. Radiometry was carried out, using a cryostat-based superconducting integrated receiver [15], on 3 subjects, for a total of 12 measurements at 500 GHz and for 30 subjects at 507 GHz for a total of 30 measurements (one of the subjects was measured in both frequencies), resulting in a pool of 32 subjects and 42 separate measurements. During the experiment at 507 GHz, the subjects were exposed to a stress protocol consisting of a 5 min calm state, 5 min of mental activity (color word test [10]), 5 min of relaxation, 2 min of physical stress (hand gripping), and finally 2 min of calm. Concurrently, the heart pulse rate and GSR, both indications of stress [18], [19], were measured.

The emitted signals were collected from a spot on the palm of the hand of 2.5 cm in diameter. The traditional lock-in amplifier scheme was employed for the data collection using a chopper for modulation [15], [17].

The voltage reading of the sensor is proportional to the brightness temperature [20] of the measured source by a sensor-scaling coefficient K

$$\mathrm{SIR}_{\mathrm{raw}}\ (t) = \ K\left[T_B\left(t\right) - T_{\mathrm{ch}}\right] \qquad (1)$$

where $\mathrm{SIR}_{\mathrm{raw}}(t)$ is the registered voltage, T_{ch} is the chopper brightness temperature, and $T_B(t)$ is the subject's brightness temperature. Two dominant factors were considered before each measurement—the ambient background and K—the absolute value of the sensor-scaling coefficient. During the experiments, the environmental conditions were kept constant and the chopper temperature can be equated to the background room temperature.

The coefficient K $[\mathrm{V}/°]$ was determined by calibration using absolute blackbody references measured at two temperatures T_{hot} and T_{cold}. The calibration measurements at these temperatures demonstrated a linear dependence of the SIR signal on the reference temperature in the range of $77\ K \leq T \leq 293.2\ K$. The sensor-scaling coefficient K could then be determined by

$$K \ = \frac{\mathrm{SIR}_{\mathrm{hot}} - \mathrm{SIR}_{\mathrm{cold}}}{T_{\mathrm{hot}} - T_{\mathrm{cold}}}. \qquad (2)$$

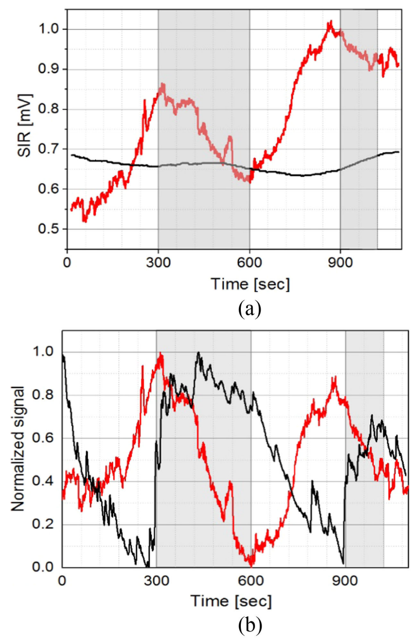

Fig. 4. (a) Representative SIR measurement for one subject. The black line represents the equivalent blackbody signal, based on the measured skin temperature of the subject, approximately 32 °C. The mental stress protocol period is shaded gray [21]. (b) Representative plot of the normalized SIR/GSR signal against time for the same subject. Compared with the GSR signal, the SIR signal was first detrended using a linear baseline [22]. SIR signal is plotted in red and the concurrent GSR signal is plotted in black. The protocol period is shaded [21].

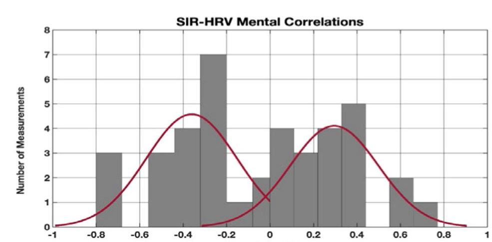

Fig. 5. Histogram of the spearman correlation between the SIR signal and the HRV for 39 measurements recorded at 500 and 507 GHz. The histogram divides into two distinct populations of the negative and positive correlation. The average correlations are 0.29 ± 0.2 and -0.36 ± 0.2. HRV is a more precise indicator of stress than GSR because it is less prone to contact problems and other artifacts. A total of 3 measurements from 42 were excluded due to incomplete pulse traces.

If the human skin acts as a perfect blackbody, then $T_B(t)$ in (1) would be equivalent to the measured palm skin temperature $T_{\mathrm{hand}}(t)$. However, we find that the measured signal is notably higher than the expected values for a blackbody held at the skin temperature, continually measured on the subject's palm throughout the protocol. A representative result is plotted in Fig. 4(a). This difference of the signal from the blackbody is repeated for all subjects. Furthermore, we find that the mental and physical stress of the subject can be correlated to changes in the measured radiometric signal, the correlations being either negative or positive.

Fig. 4(b) presents a typical result for a concurrent measurement of GSR and a radiometric SIR signal. Fig. 5 presents a histogram of the spearman correlation values [23] between the HRV, derived from the heart pulse rate measurements, and the simultaneously measured SIR signal, for all subjects.

There are two distinct populations with the average correlations of 0.29 $\pm$0.2 and -0.36 ± 0.2. While the reason for these populations is still a subject of debate, it is known that the human reactions to stressful situations fall into two categories: distress and eustress [24], [25]. One could be tempted to suggest that the two distributions are a manifestation of these categories.

Although these correlations are quite low, student's *t*-testing of the raw SIR signal before and during a period of mental stress revealed that out of 42 measurements, 36 returned a *p*-value of zero for the null hypothesis, implying that the emitted signal was substantially different during rest and during stress.

For this test, 2 sections from the SIR signal were extracted for each of the 42 measurements, one taken between 120–300 s and 0–300 s, depending on the protocol, representing the very first relaxation period, and the other representing the mental stress period, taken between 300–480 s and 300–600 s, according to the experimental protocol of each measurement. This resulted in 180–300 pairs of samples for each of the 42 measurements. The second relaxation period was not concatenated to the calm section due to the possibility that it could contain some stress artifacts. The MATLAB function, *t-test (x, y, name, value),* was used to calculate a paired student's *t*-test, with a significance value of 1% for the null hypothesis. The implication is that there is a substantial difference in the recorded signal during a calm state as opposed to a stress state. A total of 3 subjects were measured repetitively, their results rejected the null hypothesis 3 out of 4 or 5 out of 5 times.

We can conclude that this opens a new avenue for the remote monitoring of stress. While work has been done to recognize the stress by an image analysis of the human face in the THz range [26] and above [27], this is the first evidence that human stress directly affects the emission of skin.

IV. Discussion

A simple and direct representation of the experimental data can be done by binning the $\mathrm{SIR}_{\mathrm{raw}}(t)$ results into a histogram. Due to the differing sensitivities of the heterodyne at different frequencies, this can be done only for single frequencies. The result for 30 subjects at 507 GHz is plotted in Fig. 6 as the bars and the upper brightness temperature scale is calculated according to (1). One would expect that the maximum of distribution would be around the skin temperature as is common in the far infrared [28]. We find that a minimum of five Gaussian distributions are required to describe this histogram (see Fig. 6).

$$f\ (x) = \sqrt{\frac{2}{\pi}}\,\frac{A}{\sigma}\,\exp -2\left(\frac{x-\bar{x}}{\sigma}\right)^2. \tag{3}$$

The details are presented in Table I. The statistical significance of each population was established using the MATLAB function *t-test2 (x, y, "Vartype," "unequal")* for Welch's *t*-test [29]. The significance values at the α value of 0.01 are all close to zero, implying that the distributions are all statistically distinct. From the results, it is clear that population 1 is the dominant feature, comprising 46% of the total counts. It coincides with the temperature of 310 $\pm$0.5 K (37 °C), the human body core temperature. This is not an expected result, as absorption in the upper skin layers should effectively dampen any radiation produced by the core [26], [27]. The remaining four distributions are statistically distinct. However, one feels that the final fifth distribution would fold into the broad background of the first distribution given a larger sample pool. The statistical weight of the fourth distribution (*A normalized* $= 0.04$) is very low and one must question its relevance to the discussion. The second distribution (see 2-blue in Fig. 6) can be accounted for by the effect of a signal absorption inside the duct, leading to an effective lower brightness temperature. The third population is more intriguing, as it represents an effective increase in signal intensity originating from the hand of our subjects, beyond that expected by the natural variation in the blackbody signal from the human core temperature. One could speculate that this is rooted in an additional radiative source.

Furthermore, this simple approach cannot account for the signal dependence on mental stress, let alone that the core

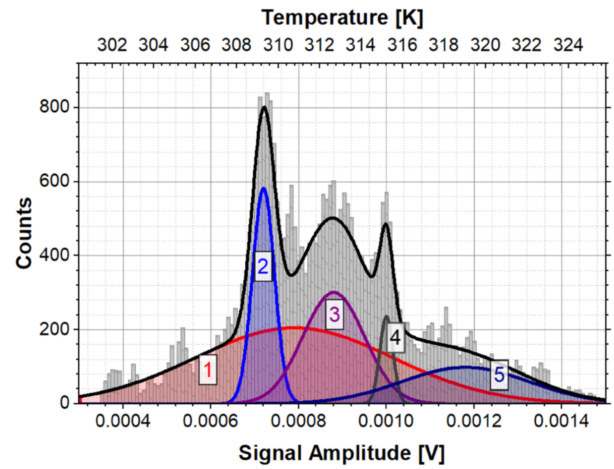

Fig. 6. Histogram of all raw SIR results for 30 subjects measured at 507 GHz. Due to differing sensitivities of the heterodyne at different frequencies, only one frequency is used. The brightness temperature scale (upper axis) assumes an average room temperature of 297 K (24 °C) and is calculated according to (1). A minimum of five Gaussian distributions (labeled 1—red, 2—blue, 3—purple, 4—dark gray, and 5—dark blue) are required to describe the histogram. Student's *t*-testing reveals statistical significance only for the distributions 1, 2 and 3. The broad distribution 1 is centered around the core temperature of the human body of 310 K (37 °C). The second and third Gaussians are situated 1 K lower and 2 K higher than the body temperature, respectively.

TABLE I
Parameters of the Gaussian Distributions Defined by (3) and Used to Describe the Histogram of Fig. 6

Distribution #	A $\times 10^{-2}$	A *normalized*	$\bar{x}$ $\times 10^{-2}$ $[V]$	σ $\times 10^{-2}$ $[V]$
1	11.56	0.46	0.079	0.045
2	3.65	0.15	0.072	0.005
3	5.28	0.21	0.088	0.014
4	0.89	0.04	0.100	0.003
5	3.58	0.14	0.118	0.029

Normalized amplitudes were calculated by $A_i^{norm} = A_i / \sum A_i$.

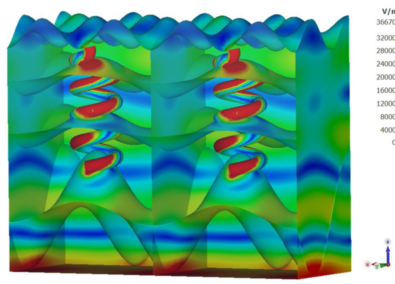

Fig. 7. Simulation model of a single sweat duct embedded in its skin layer with a radiation port (507 GHz) at its base. The colors represent the differing electromagnetic field strengths with the highest levels registered in the sweat duct.

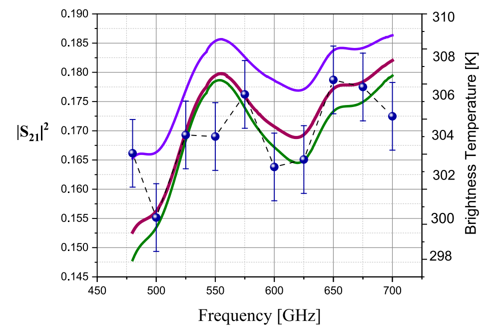

Fig. 8. Simulation of the squared modulus of the transmission coefficient $|\boldsymbol{S}_{21}(\boldsymbol{f})|^2$ proportional to transmission radiation intensity, for three different ac conductivity levels (violet - 2000 S/m, dark red - 3000 S/m, and dark green - 4000 S/m) for a source placed at the base of the epidermis in Fig. 7 as a function of frequency. On the right-hand axis is the measured SIR signal (as an equivalent brightness temperature with accuracy $\pm$ 1.7°) for a single subject of the study. The measured result and simulation are qualitatively comparable.

temperature element is a major contribution to the emission of our skin at 507 GHz. This contradicts the accepted blackbody power spectrum of the human body [26], [28].

Reflection coefficient measurements of the skin at similar frequencies also revealed a dependence on the level of human stress [30] and circular dichroism [12]. This posited the sweat duct as a major factor in the electromagnetic response of the skin at the sub-THz frequency band. One may assume similar importance of the duct in passive emissivity. To explore this concept, a simulation study was made.

The electromagnetic response of the sweat duct can be simulated by considering it as a coil embedded in a multilayered environment with the dielectric properties of the layered human skin [31], [32] (some details of the model are presented in the Appendix). The model, as illustrated in Fig. 7, consists of three layers with undulating boundaries, mimicking the papillae of human skin as noted in OCT studies [14] (see Fig. 1). Into this, a helical sweat duct with an aqueous interior is embedded. The layer electromagnetic properties were calculated by their water content, provided by Raman spectroscopy [33]. The resulting simulation led to a model that, at least in terms of a reflection coefficient, predicted a heightened radiometric response around 500 GHz [32]. The influence of stress was introduced by varying the ac conductivity in the aqueous interior of the duct. This assumption is reasonable as stress leads to heightened activity of the sweat duct, as the sympathetic nervous response is kicked into the activity [18]. As a consequence, there is an injection of charge carriers (protons) into the duct [34], effectively changing the ac conductivity. In fact, the pH levels of human sweat have been measured from 4.5 up to 7 [35], indicating a wide variation in ac conductivity levels. This mechanism would affect skin emissivity ϵ with a temperature of 27–32 °C.

However, this would not account for a blackbody signal of 37 °C. A possible explanation is that the human body core temperature produces a contribution that is measurable externally. There are strong arguments against this position as it is accepted that, in the infrared, the upper layers of the skin (the epidermis and stratum cornea) would absorb this component [26]. The transmission coefficient of the duct must be sensitive to the ac conductivity in the duct, as was the reflection coefficient [10], [11], [31], [36]. As the sweat gland, buried in the dermis, is in contact with the capillary blood system at 37 °C, the duct could influence the emission of the same blackbody signal in this frequency band. However, at a characteristic frequency of the duct, predicted by its geometry (see Fig. 7), there would be a heightened absorption of the blackbody signal. This dependence on the spiral geometry of the duct is reminiscent of the absorption characteristic of a helical antenna almost like a low-Q resonance, narrow-band notch filter [37].

In order to test this hypothesis, we have made simulation studies using the software package of computer simulation technology (CST) of the transmission coefficient (S_{21}) of the skin as a function of frequency, using our existing skin/sweat duct model [31], [32] with a radiation source embedded in the dermal layer (the details of the model are presented in the supplementary materials). Fig. 7 also shows the field distribution in the model when excited by a radiation port at the base of the spiral duct.

They confirm the ability of the skin to be a conduit for a blackbody signal at 37 °C, modulated by the activity of the duct. In order to test this hypothesis, a frequency sweep from 480 to 700 GHz was made for three subjects. The receiver was tuned and calibrated at each frequency. For the spectral measurements, a shorter protocol (5 min rest, 3 min mental stress, and 5 min rest) was used. The coefficient K was calibrated per frequency point, maximal at 500 GHz and decreased with increasing frequency. The brightness temperature $T_B(t, f)$ of each subject was evaluated as a function of frequency f using (1). The values of $T_B(t, f)$ were qualitatively compared with the results of a CST simulation of the transmission coefficient $S_{21}(f)$for a uniform source placed at the base of the epidermis below the sweat duct coil (see Fig. 7). The squared modulus $|S_{21}(f)|^2$ is proportional to the intensity of a transmitted signal and so to the brightness temperature as well. A total of three different levels of ac conductivity were simulated (2000, 3000, and 4000 S/m). The simulation results reveal an increasing value of signal with increasing frequency (see Fig. 8). This trend as well as the signal shape is maintained for each conductivity. Expressed in terms of the brightness temperature T_B, the experimental results qualitatively match the simulation. While these tendencies broadly suit a blackbody description of the radiation, one must note the dip in both the simulation and experiment around 620 GHz.

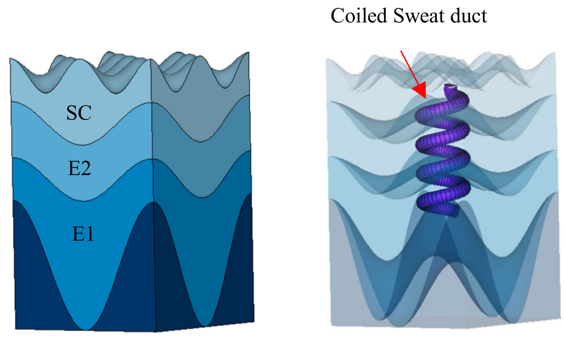

Fig. 9. Multilayered skin model. On the right, the interior of the model—the coiled sweat duct.

TABLE II
ESTIMATED SKIN DIELECTRIC PERMITTIVITY AND AC CONDUCTIVITY, WHICH WERE USED IN THE SIMULATIONS MODEL

Component	Relative Permittivity	AC Conductivity [S/m]
Stratum Cornea (SC)	2.7	0.001
Middle Epidermis (E2)	3.25	0.5
Inner Epidermis (E1)	3.8	1
Dermis	3.9	30
Sweat duct	4	2000-4000

AC conductivity of the sweat ducts is considered to be much higher than that of its surrounding epidermis.

We conclude that the human skin can be considered as an electromagnetic bio-metamaterial, capable of transmitting the human core blackbody radiation in the sub-THz range. Furthermore, the efficiency of this mechanism, reminiscent of a low-Q notch filter, is dependent on the effective ac conductivity and the morphology of the sweat duct. We speculate that the former is a product of the biochemical injection of charge carriers, itself a direct consequence of the sympathetic nerve response [18], [34], into the aqueous interior of the duct and the latter ensures a narrow frequency band of transmission. Together they offer new and intriguing avenues for medical diagnostics by making both the core temperature and the mental state of a subject available remotely.

APPENDIX

A. Model

The model is a unit cell, which consists of two main layers: dermis and epidermis. The latter is further divided into three sublayers, referred to as E1, E2, and stratum corneum (SC), from the deep most to superficial, respectively, (see Fig. 9). Although the dermis layer depth is 1–2 mm , only its upper 300 μm was considered in the model because we are interested in the "transmitted" electromagnetic (EM) field toward the skin outer surrounding. The helical section of the sweat duct was embedded in the epidermis layer to correspond with the position of the duct noted by OCT [32]. The boundary between the dermis and the epidermis was modeled as a two-dimensional (2-D) sinusoidal surface with an amplitude of 150 μm, which corresponds to the papillary dermis in the human skin [12], [14]. The moisture profile of skin as a boundary between the sublayers of the epidermis (E1 and E2) was also modeled sinusoidally with amplitudes of 50 μm. The dielectric permittivity of each layer was calculated using the mixture formula presented in [9, eq. (1)]

$$\varepsilon_{\text{layer}} = \varepsilon^{bm} \frac{\left(2\varepsilon^{bm} + \varepsilon^{w}\right) + 2x\left(\varepsilon^{bm} - \varepsilon^{w}\right)}{\left(2\varepsilon^{bm} + \varepsilon^{w}\right) + x\left(\varepsilon^{bm} - \varepsilon^{w}\right)} \quad \text{(A1)}$$

where ε^{bm} is the permittivity of the dry biological structural components, approximately 2.2 [38], ε^{w} is a permittivity of water (approximately 5 at $f = 500$ GHz [39]), and x is the volume fraction of the water component [8], [40]. In the considered frequency range, i.e., hundreds of gigahertz, dielectric losses for water are low and for the dry biological components are negligible. Consequently, the permittivity can be represented by a single frequency-independent value.

The model parameters are summarized in Table II. The ac conductivity of the sweat ducts was considered to vary from 100 (the value for pure water at 100 GHz [10]) to 4000 S/m.

B. Computational Method

The EM simulation was conducted using the CST microwave studio software package, utilizing a 3-D finite-difference or finite-element analysis to solve Maxwell's equations over a mesh of cells covering the model. We used the T-solver (time-domain solver) feature, which is based on the solution of the differential form of Maxwell's equations. The advantage of T-solver over F-solver (frequency-domain solver) is the less memory that it consumes and it is, thus, faster. The source we used is a plane wave, constructed of Floquet ports, located at the bottom of the dermis layer, and directed perpendicularly to the SC. Eventually, the transmission coefficient S_{21} was simulated at a distance of 30 cm from the plane wave source to match the experimental setup.

ACKNOWLEDGMENT

The authors would like to thank Prof. N. Bar-Gill for his valuable comments and helpful discussion. The operation of the SIR was carried out at the Kotel'nikov IRE RAS within the framework of the state task (by USU 352529).

REFERENCES

[1] C. Cajavilca and J. Varonb, "Willem Einthoven: The development of the human electrocardiogram," *Resuscitation,* vol. 76, pp. 325–328, 2008.
[2] R. Graham-Brown and T. Burns, *Lecture Notes on Dermatology*, 8 ed. Oxford, U.K.: Blackwell, 2002, p. 224.
[3] W. Li and S. Fan, "Nanophotonic control of thermal radiation for energy applications," *Opt. Exp.*, vol. 26, no. 12, pp. 15995–16021, 2018.
[4] J.-S. Fang *et al.*, "Path-dependent human identification using a pyroelectric infrared sensor and Fresnel lens arrays," *Opt. Exp.,* vol. 14, no. 2, pp. 609–624, 2006.
[5] N. M. Zainudin, S. Ramli, K. H. Ghazali, M. L. Talib, and N. A. Hasbullah, "A study on implementing physiology-based approach and optical flow algorithm to thermal screening system for flu detection," *Int. J. Inf. Electron. Eng.,* vol. 5, no. 1, pp. 31–34, 2015.

[6] A. Y. Owda, N. Salmon, and N. D. Rezgui, “Electromagnetic signatures of human skin in the millimeter wave band 80–100 GHz,” *Prog. Electromagn. Res. B,* vol. 80, pp. 79–99, 2018.

[7] K. Baksheeva *et al.*, “Study of human skin radiation in the terahertz frequency range,” *J. Phys., Conf. Ser.*, vol. 1410, 2019, Art. no. 012076.

[8] Y. Feldman, A. Puzenko, P. Ben Ishai, A. Caduff, and A. J. Agranat, “Human skin as arrays of helical antennas in the millimeter and submillimeter wave range,” *Phys. Rev. Lett.,* vol. 100, Mar. 28, 2008, Art. no. 128102.

[9] Y. Feldman *et al.*, “The electromagnetic response of human skin in the millimetre and submillimetre wave range,” *Phys. Med. Biol.*, vol. 54, pp. 3341–3363, 2009.

[10] E. Safrai *et al.*, “The remote sensing of mental stress from the electromagnetic reflection coefficient of human skin in the sub-THz range,” *Bioelectromagnetics*, vol. 33, pp. 375–382, 2012.

[11] A. Kochnev, N. Betzalel, P. Ben Ishai, and Y. Feldman, “Human sweat ducts as helical antennas in the sub-THz frequency range—An overview,” *Terahertz Sci. Technol.*, vol. 11, pp. 43–56, 2018.

[12] I. Hayut, P. Ben Ishai, A. J. Agranat, and Y. Feldman, “Circular polarization induced by the three-dimensional chiral structure of human sweat ducts,” *Phys. Rev. E,* vol. 89, Apr. 25, 2014, Art. no. 042715.

[13] A. Knuttel, S. Bonev, and W. Knaak, “New method for evaluation of in vivo scattering and refractive index properties obtained with optical coherence tomography,” *J. Biomed. Opt.*, vol. 9, no. 2, pp. 265–273, 2004.

[14] S. R. Tripathi, E. Miyata, P. Ben Ishai, and K. Kawase, “Morphology of human sweat ducts observed by optical coherence tomography and their frequency of resonance in the terahertz frequency region,” *Sci. Rep.*, vol. 5, 2015, Art. no. 9071.

[15] V. P. Koshelets and S. V. Shitov, “Integrated superconducting receivers,” *Supercond. Sci. Technol.*, vol. 13, pp. R53–R69, 2000.

[16] G. de Lange *et al.*, “Development and characterization of the superconducting integrated receiver channel of the TELIS atmospheric sounder,” *Supercond. Sci. Technol.,* vol. 23, no. 4, 2010, Art. no. 045016.

[17] V. P. Koshelets *et al.*, “Superconducting integrated terahertz spectrometers,” *IEEE Trans. Terahertz Sci. Technol.,* vol. 5, no. 4, pp. 687–694, Jul. 2015.

[18] J. T. Cacioppo, L. G. Tassinary, and G. G. Berntson, *Handbook of Psychophysiology*. Cambridge, MA, USA: Cambridge Univ. Press, 2007, p. 898.

[19] J. Zhai and A. Barreto, “Stress detection in computer users through non-invasive monitoring of physiological signals,” *Biomed. Sci. Instrum.*, vol. 42, pp. 495–500, 2006.

[20] G. B. Rybicki and A. P. Lightman, *Radiative Processes in Astrophysics*. New York, NY, USA: Wiley, 1991, p. 382.

[21] K. A. Baksheeva *et al.*, “Do humans ‘shine’ in the sub THz?” *presented at the 44th Int. Conf. Infrared, Millimeter, Terahertz Waves*, Paris, France, 2019.

[22] A. de Cheveigne and D. Arzounian, “Robust detrending, rereferencing, outlier detection, and inpainting formultichannel data,” *Neuroimage,* vol. 172, pp. 903–912, 2018.

[23] J. L. Myers and A. D. Well, *Research Design and Statistical Analysis*, 2nd ed. Mahwah, NJ, USA: Lawrence Erlbaum, 2003, p. 508.

[24] M. Le Fevre, J. Matheny, and G. S. Kolt, “Eustress, distress, and interpretation in occupational stress,” *J. Managerial Psychol.,* vol. 18, no. 7, pp. 726–744, 2003.

[25] J. Lefevre, “Teleonomical optimization of a fractal model of the pulmonary arterial bed,” *J. Theor. Biol.*, vol. 102, no. 2, pp. 225–248, 1983.

[26] K. Leijon-Sundqvist, Y. Tegner, U. Juntti, K. Karp, and N. Lehto, “Hand skin temperature—Are there warm and cold rewarming patterns after cold stress test?” *Thermol. Int.,* vol. 26, no. 3, pp. 81–87, 2016.

[27] J. McGowan, D. Gardner, and R. Fletcher, “Positive and negative affective outcomes of occupational stress,” *New Zealand J. Psychol.*, vol. 35, no. 2, pp. 92–98, 2006.

[28] A. Y. Owda *et al.*, “Millimeter-wave emissivity as a metric for the non-contact diagnosis of human skin conditions,” *Bioelectromagnetics,* vol. 38, pp. 559–569, 2017.

[29] G. D. Ruxton, “The unequal variance t-test is an underused alternative to student’s t-test and the Mann–Whitney U test,” *Behav. Ecol.*, vol. 17, no. 4, pp. 688–690, 2006.

[30] A. Kochnev, A. Puzenko, P. Ben Ishai, and Y. Feldman, “Electromagnetic reflectance measurements of human palms in sub-THz frequency band,” presented at the 44th Int. Conf. Infrared, Millimeter, Terahertz Waves, Paris, France, Sep. 1–6, 2019.

[31] I. Hayut *et al.*, “The helical structure of sweat ducts: Their influence on the electromagnetic reflection spectrum of the skin,” *IEEE Trans. Terahertz Sci. Technol.,* vol. 3, no. 2, pp. 207–215, Mar. 2013.

[32] N. Betzalel, Y. Feldman, and P. Ben Ishai, “The modeling of the absorbance of sub-THz radiation by human skin,” *IEEE Trans. Terahertz Sci. Technol.*, vol. 7, no. 5, pp. 521–528, Sep. 2017.

[33] M. Egawa, T. Hirao, and M. Takahashi, “In vivo estimation of stratum corneum thickness from water concentration profiles obtained with Raman spectroscopy,” *Acta Dermato Venereologica,* vol. 87, no. 1, pp. 4–8, 2007.

[34] Z. Sonner *et al.*, “The microfluidics of the eccrine sweat gland, including biomarker partitioning, transport, and biosensing implications,” *Biomicrofluidics*, vol. 9, 2015, Art. no. 031301.

[35] H. Lambers, S. Piessens, A. Bloem, H. Pronk, and P. Finkel, “Natural skin surface pH is on average below 5, which is beneficial for its resident flora,” *Int. J. Cosmetic Sci.,* vol. 28, pp. 359–370, 2006.

[36] E. Safrai, P. Ben Ishai, A. Polsman, S. Einav, and Y. Feldman, “The correlation of ECG parameters to the sub-THz reflection coefficient of human skin,” *IEEE Trans. Terahertz Sci. Technol.*, vol. 4, no. 5, pp. 624–630, Sep. 2014.

[37] M. Yu and V. Dokas, “High performance helical resonator filters,” presented at the 34th Eur. Microw. Conf., Amsterdam, The Netherlands, Oct. 12–14, 2004.

[38] R. Pethig, “Dielectric properties of body tissues,” *Clin. Phys. Physiol. Meas.*, vol. 8, no. 4A, pp. 5–12, 1987.

[39] W. J. Ellison, “Permittivity of pure water, at standard atmospheric pressure, over the frequency range 0–25THz and the temperature range,” *J. Phys. Chem. Ref. Data,* vol. 36, no. 1, pp. 1–18, 2007.

[40] R. R. Pethig, *Dielectric and Related Molecular Processes*, vol. 3, M. Davies, Ed. London, U.K.: The Chemical Society, 1977.

Ksenia A. Baksheeva received the B.S. and M.S. degrees in physics from Moscow State Pedagogical University, Moscow, Russia, in 2015 and 2017, respectively, where she is currently working toward the Ph.D. degree in radiophysics.

She is currently a Junior Researcher with the Laboratory of Quantum Detectors, Moscow State Pedagogical University.

Roman V. Ozhegov received the M.S. degree in physics from Vyatka State Pedagogical University, Kirov, Russia, in 2002, and the Ph.D. degree in radiophysics from Moscow State Pedagogical University (MSPU), Moscow, Russia, in 2011.

He is currently a Senior Researcher with the Laboratory of Quantum Detectors, MSPU. His scientific interests include superconductivity, quantum optics, and quantum-integrated optics.

Gregory N. Goltsman was born in Moscow. He received the Ph.D. degree in physics of semiconductors and the Sc.D. degree in semiconductor and dielectric physics from Moscow State Pedagogical University (MSPU), Moscow, Russia, in 1973 and 1985, respectively.

He is currently a Professor with the Department of Physics and Information Technology, MSPU, where he is also the Head of the Radiophysics Research and Educational Center. His scientific interests include superconductivity, nonequilibrium phenomena in superconductors, semiconductors, quantum optics, quantum-integrated optics, far-infrared spectroscopy, as well as terahertz direct detectors and mixers. He is the Author and Co-Author of more than 450 papers published in several journals and conference proceedings.

Nickolay V. Kinev received the B.S. degree in applied mathematics and physics and the M.S. degree in solid-state electronics and radiophysics from the Moscow Institute of Physics and Technology, Moscow, Russia, in 2007 and 2009, respectively, and the Ph.D. degree in radiophysics from the Kotel'nikov Institute of Radio Engineering and Electronics, Russian Academy of Sciences, Moscow, Russia, in 2013.

He is currently a Senior Researcher with the Kotel'nikov Institute of Radio Engineering and Electronics, Russian Academy of Sciences, Moscow, Russia. His research interests include superconducting receivers and oscillators for terahertz technologies and space applications.

Dr. Kinev was a recipient of the Government of Moscow Young Scientist Award in 2018 for the contribution to the study of superconducting terahertz sources.

Valery P. Koshelets (Member, IEEE) received the M.S. degree in physics from Lomonosov Moscow State University, Moscow, Russia, in 1973, the Ph.D. degree in radiophysics and the Doctor of Sciences (Habilitation) degree in physical electronics from the Kotel'nikov Institute of Radio Engineering and Electronics (IREE), Russian Academy of Sciences, Moscow, Russia, in 1978 and 1990, respectively.

Since 1973, he has been with Kotel'nikov IREE, where he is currently the Head of the Laboratory of superconducting devices for signal detection and processing.

Anna Kochnev received the B.Sc. degree in electrical and computer engineering in 2015 and the M.Sc. degree in applied physics in 2018, both from The Hebrew University of Jerusalem, Jerusalem, Israel.

Her research with the laboratory of Prof. Y. Feldman included developing a microwave antenna for small tumor ablation in the digestive system and studying the electromagnetic response of the human skin in the sub-THz frequency range. In addition to this academic background, she has six years of experience working in the industry as a Software Engineer with Intel Corp., Santa Clara, CA, USA, designing and developing various software solutions for numerous clients. She is passionate about utilizing engineering, physics, and programming to achieve advances in medicine and healthcare.

Noa Betzalel received the B.Sc. degree in electrical and computer engineering specialized in microelectronics and optoelectronics, and the M.Sc. degree in applied physics from the Faculty of Natural Sciences, The Hebrew University of Jerusalem, Jerusalem, Israel, where she is currently working toward the Ph.D. degree with the Department of Applied Physics, Faculty of Sciences.

Her research interests include medical physics, biophysics, and sub-THz frequencies technologies.

Alexander Puzenko received the M.Sc. degree in radiophysics and electronics and the Ph.D. degree in radiophysics and quantum radiophysics from Kharkov State University, Kharkiv, Ukraine, in 1966 and 1979, respectively.

From 1966 to 1983, he was with the Department of Radio Waves Propagation and Ionosphere, Institute of Radiophysics and Electronics, Ukrainian Academy of Sciences, Kharkov. From 1984 to 1994, he was a Senior Scientist with the Department of Space Radiophysics, Institute of Radio Astronomy National Academy of Science, Kharkov. In 1995, he immigrated to Israel, and since 1997, he has been with The Hebrew University of Jerusalem, Jerusalem, Israel, where he is currently a Senior Scientist with Dielectric Spectroscopy Laboratory, Department of Applied Physics. His current research interests include time- and frequency-domain broadband dielectric spectroscopy, theory of dielectric polarization, relaxation phenomena, and strange kinetics in disordered materials, transport properties and percolation in complex systems, dielectric properties of biological systems, and electromagnetic properties of human skin in the sub-THz frequency range.

Paul Ben Ishai received the Ph.D. degree in applied physics from the Hebrew University of Jerusalem, Jerusalem, Israel, in 2009.

He is currently a Senior Lecturer with the Department of Physics, Ariel University, Ariel, Israel, and the Head of the Laboratory of Terahertz Dielectric Spectroscopy. He was the Director of the Hebrew University's Center for Electromagnetic Research and Characterization, Department of Applied Physics. Until 2016, he was involved with the Laboratory of Prof. Feldman, concentrating on dielectric research. His research interests include soft condensed matter physics, glassy dynamics, biophysics, sub-terahertz spectroscopy, and dielectric spectroscopy.

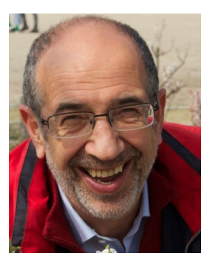

Yuri Feldman received the M.S. degree in radiophysics and the Ph.D. degree in molecular physics from Kazan State University, Kazan, Russia, in 1973 and 1981, respectively.

From 1973 to 1991, he was with the Laboratory of Molecular Biophysics, Kazan Institute of Biology, Academy of Science, Kazan, Russia. In 1991, he immigrated to Israel, and since 1991, he has been with the Hebrew University of Jerusalem, Jerusalem, Israel, where he is currently a Full Professor and the Head of the Laboratory of Soft Condensed Matter. He is also the Director of the Center for Electromagnetic Research and Characterization. His current interests include broadband dielectric spectroscopy in frequency and time domain, theory of dielectric polarization and relaxation, relaxation phenomena and strange kinetics in disordered materials, and electromagnetic properties of biological systems *in vitro* and *in vivo*.